Intramolecular Energy Transfer in Covalently Linked Polypyridine Ruthenium(II)/Osmium(II) Binuclear Complexes. $Ru(II)(bpy)_2Mebpy-(CH_2)_n-MebpyOs(II)(bpy)_2$ (n=2, 3, 5, and 7)

Masaoki FURUE,* Toshiyuki YOSHIDZUMI, Shuichi KINOSHITA,†,†† Takashi KUSHIDA,† Shun-ichi NOZAKURA, and Mikiharu KAMACHI
Department of Macromolecular Science, Faculty of Science, Osaka University, Toyonaka, Osaka 560
† Department of Physics, Faculty of Science, Osaka University, Toyonaka, Osaka 560
(Received November 19, 1990)

A novel series of polymethylene-linked heterobinuclear complexes of polypyridine ruthenium(II)/osmium(II) complex $Ru(II)(bpy)_2Mebpy-(CH_2)_n-MebpyOs(II)(bpy)_2$(bpy=2,2′-bipyridine and n=2, 3, 5, and 7), **1**, was prepared. The photophysical behavior was examined in various solvents. The emission spectra of **1** (excitation wavelength: 455nm) showed a nearly complete quenching of $Ru^{II}\rightarrow\pi^*$(bpy) metal-to-ligand charge transfer (MLCT) emission and the enhancement of $Os^{II}\rightarrow\pi^*$(bpy) MLCT emission. The luminescence lifetime measurements by a time-correlated single photon-counting method provided evidence that intramolecular energy transfer is a significant pathway for the observed emission quenching. The rate constants of the intramolecular energy transfer in ethanol are 5.3×10^8, 3.3×10^8, 1.3×10^8, and $1.0\times10^8 s^{-1}$ for **1**(n=2, 3, 5, and 7), respectively. They were found to be proportional to the inverse sixth power on the center-to-center distance of the two complexes. The mechanism is discussed in terms of the Förster (a dipole–dipole interaction) mechanism.

There has been considerable interest in photochemical and photophysical processes of molecular assemblies consisting of polypyridine and porphyrin complexes of the transition metals.[1-5] A possible use of these materials is to control photochemical processes in which optical excitation is followed by spatially directed energy or electron transfer.[6-10] We have studied the photochemical and photophysical properties of $Ru(bpy)_3^{2+}$-containing polymers in which $Ru(bpy)_3^{2+}$ complexes are covalently incorporated into poly(4-methyl-4′-vinyl-2,2′-bipyridine).[11] In our recent study, covalently linked dimers of $Ru(bpy)_3^{2+}$ (complex **2**) as a dimer model for $Ru(bpy)_3^{2+}$-containing polymers exhibited rather different photophysical behaviors in comparison with those of aromatic hydrocarbon and porphyrin dimers.[12-15] In excited **2**, no intramolecular interaction leading to the enhanced quenching between the excited and ground states was found. However, an efficient intramolecular triplet–triplet annihilation process was found under the high intensity irradiation of laser light.[16] These results aroused our interest in the heterobinuclear system.

The intramolecular energy-transfer processes in a variety of weakly coupled dimers of transition metal complexes have been the subjects of both theoretical and mechanistic studies.[17-20] Two major mechanisms for energy transfer in organic systems have been recognized.[21,22] Energy transfer can take place via a dipole–dipole interaction between an electronically excited donor and an acceptor in the ground state (i.e., the Förster mechanism).[23] The other mechanism involved in energy transfer is an electron-exchange mechanism in which a spatial overlap of the donor and acceptor is required (i.e., the Dexter mechanism).[24] Since electronic transition in transition metal complexes are frequently symmetry and spin forbidden, the Förster-type energy transfer based on a dipole–dipole interaction is usually unimportant in these systems. However, it cannot be dismissed for some transition metal complexes. An appreciable amount of singlet character in luminescent excited states of $Ru(bpy)_3^{2+}$ and $Os(bpy)_3^{2+}$ has been recognized.[25,26] There are a few examples of binuclear complexes for which the Förster mechanism is conceivable in the excited state. Schmehl has discussed the intramolecular energy transfer of covalently linked ruthenium(II) dimers in terms of a dipolar coupling mechanism, namely the Förster mechanism.[18] We have also discussed the intramolecular energy transfer of a heterobinuclear complex of polypyridine–ruthenium(II) and –osmium(II), (complex **3**) using the Förster mechanism.[27]

The Förster and Dexter mechanisms are typically distinguished by evaluating the dependence of the rate of energy transfer on the distance of donor–acceptor separation. The dependence of the inverse sixth power of the distance is expected for a dipole–dipole coupling process, while an exponential dependence of distance is observed for the Dexter mechanism. There has been no systematic examination of the distance dependency of energy transfer for covalently linked complexes of this type.

We have recently established a synthetic method regarding polymethylene linked dimers of 4-methyl-2,2′-bipyridine. This work presents 1) the preparation of the ligand dimers and a novel series of polymethylene-linked heterobinuclear complexes comprising the polypyridine ruthenium(II)/osmium(II) complex $Ru(II)(bpy)_2Mebpy-(CH_2)_n-MebpyOs(II)(bpy)_2$ (bpy=2,2′-bipyridine, n=2,3,5 and 7), **1**,

2) their spectroscopic and electrochemical properties,

†† Present Address: Research Institute of Applied Electricity, Hokkaido University, Sapporo 060.

and

3) a kinetic study of intramolecular energy transfer in excited **1** by a time-correlated single-photon counting method. For these complexes, the rate constant of the intramolecular energy transfer (k_{en}) decreases with increasing number of methylene chains. The results are elucidated by the Förster mechanism. Electron localization in the excited MLCT state of the ruthenium part is also discussed in conjunction with the results for Ru(II)(bpy)$_2$Mebpy–[CH$_2$CH(OH)CH$_2$]–MebpyOs(II)-(bpy)$_2$, **3** and Ru(II)(Me$_2$bpy)$_2$Mebpy–[CH$_2$CH(OH)CH$_2$]–MebpyOs(II)(bpy)$_2$, **4**.

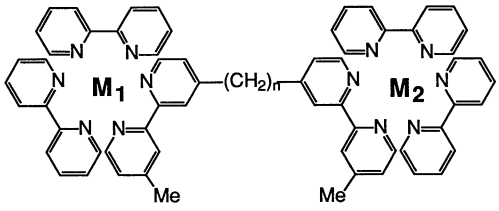

1: M_1 = Ru(II), M_2 = Os(II), n=2,3,5,7

2: M_1 = M_2 = Ru(II), n=2,3,5

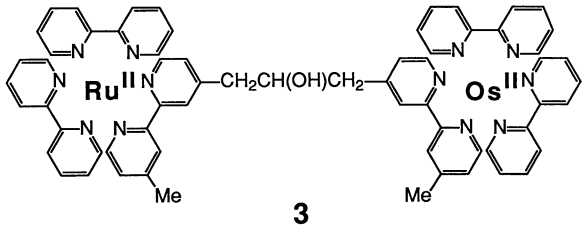

3

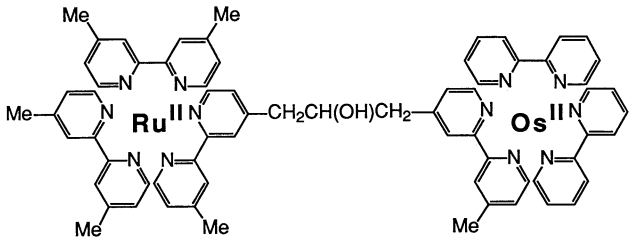

4

Experimental

Materials. The synthesis of **1** is outlined in Scheme 1. The starting material, 4,4′-dimethyl-2,2′-bipyridine, was purchased from Tokyo Kasei and recrystallized from ethanol.

4-Methyl-2,2′-bipyridine-4′-carbaldehyde (7). A mixture of 4,4′-dimethyl-2,2′-bipyridine (12.5 g, 68 mmol) and selenium dioxide (7.52 g, 68 mmol) in diglyme (120 ml) was stirred at 130—135 °C for 6 h. The reaction mixture was dissolved in 1 l of hot water and filtered to remove selenium metals. The filtrate was adjusted to pH 9—10 with an aqueous NaOH solution (10%) and extracted four times with 300 ml of the $CHCl_3$ portions. The extract was dried ($MgSO_4$) and evaporated to give a pale-yellow solid. Column chromatography on silica gel (ethyl acetate) affored a white solid **7** (5.3 g, 40%), mp 135—136 °C: ^{1}H NMR ($CDCl_3$) δ=2.5(s, 3H), 7.0—9.0(m, 6H), 10.3 (s, 1H); IR (Nujol) 1710 cm^{-1}. Anal. Calcd for $C_{12}H_{10}N_2O$: C, 72.71; H, 5.08; N, 14.13. Found: C, 72.74; H, 5.11; N, 14.03%.

4-Hydroxymethyl-4′-methyl-2,2′-bipyridine (8a). A solution of **7** (5.3 g, 27 mmol) and sodium borohydride (3 g, 79 mmol) in anhydrous ethanol (350 ml) was stirred at room temperature for 1.5 h. Water (300 ml) was then added dropwise, and the mixture stirred at room temperature overnight. The solution was then extracted with $CHCl_3$ (4×300 ml). The extract was dried ($MgSO_4$) and evaporated to give a white solid. Recrystallization from ethanol provided 4.5 g (84%) of **8a**, mp 124—125 °C: ^{1}H NMR ($CDCl_3$) δ=2.4 (s, 3H), 3.9—4.6 (s, 1H), 4.7 (s, 2H), 7.0—8.6 (m. 6H); IR (Nujol) 3200 cm^{-1}. Anal. Calcd for $C_{12}H_{12}N_2O$: C, 71.98; H, 6.04; N, 13.99%. Found: C, 72.27; H, 6.08; N, 13.98%.

4-Bromomethyl-4′-methyl-2,2′-bipyridine (9a). A mixture of **8a** (2.0 g, 10 mmol) and thionyl bromide (5 ml, 63 mmol) in 25 ml of CH_2Cl_2 was stirred at room temperature for 3 h under the flow of nitrogen gas. Water (200 ml) was added. The reaction mixture was neutralized (pH 8—9) with a saturated Na_2CO_3 solution and extracted with 500 ml of CH_2Cl_2.

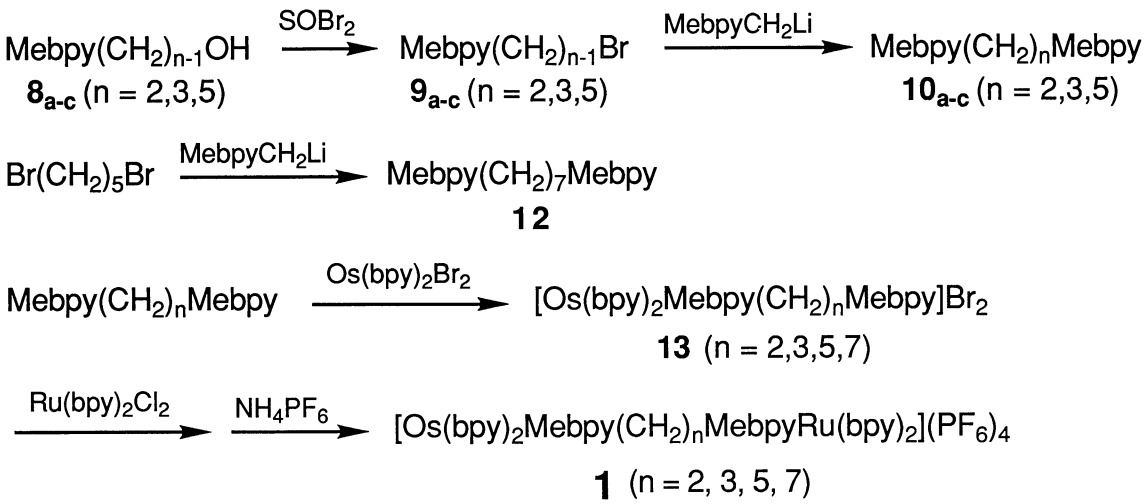

Scheme 1.

After the extract was dried ($MgSO_4$) and evaporated below room temperature, the crude product was chromatographed on a silica-gel column by eluting with ethyl acetate–CH_2Cl_2 (3:2) to give 0.78 g (30%) of white crystals of **9a**, mp 76—77 °C: ^1H NMR ($CDCl_3$) δ=2.4 (s, 3H), 4.5 (s, 2H), 7.0—8.8 (m, 6H). Anal. Calcd for $C_{12}H_{11}N_2Br$: C, 54.77; H, 4.21; N, 10.65%. Found; C, 54.48; H, 4.21; N, 10.56%.

Lithiation of 4,4′-Dimethyl-2,2′-bipyridine. To a solution of 4,4′-dimethyl-2,2′-bipyridine (3.4 g, 18 mmol) in 200-ml of THF, lithium diisopropylamide (12 mmol) in THF (10 ml) was added at 0 °C under an argon atmosphere. After the solution was stirred for 1.5 h it was ready for subsequent steps.

1,2-Bis(4′-methyl-2,2′-bipyridyl-4-yl)ethane (10a). To a stirred solution of lithiated 4,4′-dimethyl-2,2′-bipyridine, **9a** (2.0 g, 7.6 mmol) in 70 ml of THF was added dropwise at room temperature. The mixture was stirred for 1 h. Methanol (10 ml) and then water (100 ml) were added. The resulting solution was extracted with 1 l of ether. The extract was dried ($MgSO_4$) and evaporated. The residue was placed on a silica gel column, eluted with a gradient mixture of ethyl acetate–CH_2Cl_2 from 1:9 to 3:1 to remove any 4,4′-dimethyl-2,2′-bipyridine and unidentified by-products, and with methanol to provide a white solid of **10a**. Recrystallization from ethanol yielded 1.4 g (50%) of **10a**, mp 198—199 °C: ^1H NMR ($CDCl_3$) δ=2.5 (s, 6H), 3.2 (s, 4H), 7.0—9.0 (m, 6H). Anal. Calcd for $C_{24}H_{22}N_4$: C, 78.66; H, 6.05; N, 15.29%. Found: C, 78.66; H, 6.05; H, 15.23%.

4-(2-Bromoethyl)-4′-methyl-2,2′-bipyridine (9b). Using 4-(2-hydroxyethyl)-4′-methyl-2,2′-bipyridine, **8b**[28] (3.0 g, 14 mmol) and thionyl bromide (7.5 ml, 95 mmol) as the starting materials, the reaction was worked up using the procedure described regarding the preparation of **9a**. It provided 1.8 g (46%) of **9b** as a clear oil: ^1H NMR ($CDCl_3$) δ=2.4 (s, 3H), 3.2 (t, 2H), 3.6 (t, 2H), 7.0—8.7 (m, 6H). Anal. Calcd for $C_{13}H_{13}N_2Br$: C, 56.52; H, 4.71; N, 10.07%. Found; C, 56.52; H, 4.82; N. 10.15%.

1,3-Bis(4′-methyl-2,2′-bipyridyl-4-yl)propane (10b). 10b was prepared from **9b** (1.3 g, 5 mmol) by the same procedure described regarding the preparation of **10a**. 4-Methyl-4′-vinyl-2,2′-bipyridine (0.3 g) as a by-product was obtained from the early eluates. Yield of **10b** was 1.2 g (63 %), mp 128 °C: ^1H NMR ($CDCl_3$) δ=2.1 (q, 2H), 2.4 (s, 6H), 2.8 (t, 4H), 7.0—8.7 (m, 12H). Anal. Calcd for $C_{25}H_{24}N_4$; C, 79.04; H, 6.32; N, 14.64%. Found: C, 78.71; H, 6.41; N, 14.61%.

1,3-Bis(4′-methyl-2,2′-bipyridyl-4-yl)-2-propanol (11). Ethyl formate (0.88 ml, 12 mmol) was added dropwise to a solution of monolithiated 4,4′-dimethyl-2,2-bipyridine (30 mmol) in 150 ml of THF at room temperature. The mixture was stirred overnight at room temperature, quenched with 150 ml of water, neutralized (pH 8—9) with 10% (v/v) methanolic HCl, and extracted four times with 100 ml $CHCl_3$ portions. The extracts were dried ($MgSO_4$) and evaporated to give a brownish-yellow solid. Purification of the crude product was achieved through several recrystallizations from methanol to provide a white solid **11** in a yield of 20%, mp 159—160 °C. ^1H NMR ($CDCl_3$) δ=2.45 (s, 6H), 2.93 (dd, 4H), 4.33 (m, 1H), 7.12—8.54 (m, 12H), MS m/z 396. Anal. Calcd for $C_{25}H_{24}NO$: C, 75.73; H, 6.10; N, 14.13%. Found: C, 75.93; H, 6.12; N, 13.97%.

4-(4-Hydroxybutyl)-4′-methyl-2,2′-bipyridine (8c). To a solution of lithiated 4,4′-dimethyl-2,2′-bipyridine (48 mmol), 1-bromo-3-(tetrahydro-2-pyranyloxy)propane[29] (10 g, 45 mmol) in 70-ml of THF was added dropwise. The resulting mixture was stirred overnight at room temperature. Methanol (10 ml) and then water (100 ml) were added. The solution was extracted with 1 l of chloroform. The extract was dried ($MgSO_4$) and evaporated. The residue was placed on an alumina column and eluted with benzene to provide 11.7 g of 4-methyl-4′-[4-(tetrahydro-2-pyranyloxy)butyl]-2,2′-bipyridine. ^1H NMR ($CDCl_3$) δ=1.4—1.8 (m, 10H), 2.4 (s, 3H), 2.7 (t, 2H), 3.3—4.0 (m, 4H), 4.6 (t, 2H), 7.0—8.6 (m, 6H). 4-Methyl-4′-(4-tetrahydropyran-2-yloxybutyl)-2,2′-bipyridine (11.7 g) in 300 ml of ethanol was treated with *p*-toluenesulfonic acid to give 3.3 g (30%) of **8c**. ^1H NMR ($CDCl_3$) δ=1.7 (m, 4H), 2.4 (s, 3H), 2.7 (t, 2H), 3.6 (t, 2H), 7.1—8.6 (m, 6H).

4-(4-Bromobutyl)-4′-methyl-2,2′-bipyridine (9c). A mixture of **8c** (3.5 g, 14 mmol) and thionyl bromide (25 g, 120 mmol) in 30 ml of CH_2Cl_2 was stirred at room temperature for 3 h under the flow of nitrogen gas. Water (200 ml) was added. The reaction mixture was neutralized (pH 8—9) with an aqueous solution saturated with Na_2CO_3 and extracted with 500 ml of CH_2Cl_2. After the extract was dried ($MgSO_4$) and evaporated below room temperature, the crude product was chromatographed on a silica-gel column by eluting with ethyl acetate–CH_2Cl_2 (3:2) to give 3.7 g (84%) of **9c**. ^1H NMR ($CDCl_3$): δ=1.8 (m, 4H), 2.4 (s, 3H), 2.7 (t, 2H), 3.4 (t, 2H), 7.1—8.6 (m, 6H).

1,5-Bis(4′-methyl-2,2′-bipyridyl-4-yl)pentane (10c).[30] To a solution of lithiated 4,4′-dimethyl-2,2′-bipyridine (24 mmol), **9c** (3.7 g, 12 mmol) in 30 ml of THF was added dropwise at room temperature. Methanol(10 ml) and then water (100 ml) were added. The resulting solution was extracted with 1 l of chloroform. The extract was dried ($MgSO_4$) and evaporated. The residue was placed on a silica gel column and eluted with a mixture of acetone–CH_2Cl_2 (1:9 v/v) to provide a white solid of **10c**. Recrystallization from methanol yielded 2.4 g (48 %) of **10c**, mp 115—116 °C; ^1H NMR ($CDCl_3$) δ=1.3—1.9 (m, 6H), 2.4 (s, 6H), 2.7 (t, 4H), 7.1—8.6 (m, 12H), MS m/z 408. Anal Calcd for $C_{27}H_{28}N_4$: C, 79.38; H, 6.91; N, 13.71%. Found: C, 79.40; H, 6.84; N, 13.70%.

1,7-Bis(4′-methyl-2,2′-bipyridyl-4-yl)heptane (12). To a solution of lithiated 4,4′-dimethyl-2,2′-bipyridine (27 mmol), 1,5-dibromopentane (1.85 ml, 14 mmol) was added dropwise at room temperature. The mixture was stirred for 20 h. The solution was quenched with methanol and neutralized with methanol–HCl. The reaction mixture was diluted with 100 ml of water and extracted with dichloromethane. The extract was dried ($MgSO_4$) and evaporated. The residue was placed on a silica-gel column and eluted with a mixture of CH_2Cl_2–acetone (9:1, v/v) to give a white solid. Recrystallization from ethanol yielded 2.2 g (37%) of **12**, mp 86—87 °C: ^1H NMR ($CDCl_3$) δ=1.36 (m, 6H), 1.69 (q, 4H), 2.43 (s, 6H), 2.67 (t, 4H), 7.11 (d, 4H), 8.21 (s, 4H), 8.53 (dd, 4H). Anal. Calcd for $C_{29}H_{32}N_4$: C, 79.78; H, 7.39; N, 12.83%. Found: C, 79.62, H, 7.36; N, 12.66%.

$Os(II)(bpy)_2$Mebpy-$(CH_2)_n$-Mebpy (13) and $Ru(II)(bpy)_2$-Mebpy-$(CH_2)_n$-Mebpy$Os(II)(bpy)_2(PF_6)_4$ (1). Compound **13** was obtained by refluxing a mixture (10:1) of α,ω-bis(4′-methyl-2,2′-bipyridyl-4-yl)alkane and $Os(bpy)_2Br_2$ in methanol for 24 h. After the isolation of **13** by chromatography on a Sephadex LH-20 with a methanol eluent, treatment of **13** with $Ru(bpy)_2Cl_2$ in methanol under reflux, and then with ammonium hexafluorophosphate in water, afforded **1**. Compound **1** was purified by the same procedure with **13** and was recrys-

tallized from water as a PF_6^- salt.

Ru(II)(bpy)$_2$Mebpy-[CH$_2$CH(OH)CH$_2$]-MebpyOs(II)(bpy)$_2$ (3) and **Ru(II)(Me$_2$bpy)$_2$Mebpy-[CH$_2$CH(OH)CH$_2$]-MebpyOs(II)(bpy)$_2$, (4).** Compounds **3** and **4** were prepared from **11**, Os(bpy)$_2$Br$_2$, and Ru(bpy)$_2$Cl$_2$ (or Ru(Me$_2$bpy)$_2$Cl$_2$), according to the procedure described for **1**.

Measurements. Samples for luminescence measurements were deoxygenated by purging with argon gas. Solvents for spectroscopic measurements were purchased from Nakarai Chemicals as in spectrograde. Static absorption and luminescence measurements were performed using a Shimadzu UV-2100 spectrometer and an RF-502A spectrofluorimeter, respectively. The luminescence lifetime was measured by the time-correlated single photon counting method, as described elsewhere.[31] The luminescence lifetimes for the complexes at room temperature are listed in Table 1; the reported lifetimes represent the average of several independent determinations. Electrochemical measurements were performed in a conventional single-compartment cell equipped with a glassy carbon or platinum working electrode and a saturated calomel electrode as a reference electrode (SCE). All measurements were carried out using a NF function generator (FG-12113) and a Hokuto Potentiostat (HA-301) at a scan rate 0.2V s^{-1}. Tetrabutylammonium perchlorate (TBAP) was used as the supporting electrolyte and acetonitrile as the solvent. The sample solution (1 mM, 1 M=1 mol dm^{-3}) was deaerated by bubbling with argon gas.

Results and Discussion

The bridging ligand was first coupled with 1/10 equimolar Os(bpy)$_2$Br$_2$ and purified by repeated Sephadex LH-20 chromatography to remove any unreacted bridging ligand and Os(II)(bpy)$_2$Mebpy-(CH$_2$)$_n$-MebpyOs(II)-(bpy)$_2$. Treatment of Os(II)(bpy)$_2$Mebpy-(CH$_2$)$_n$-Mebpy with Ru(bpy)$_2$Cl$_2$ and ammonium hexafluorophosphate afforded **1** as a PF_6 salt. Purification of **1** was achieved by repreated chromatography using Sephadex LH-20 methanol as an eluent. On the basis of lifetime measurements, the possible existence of Ru(II)(bpy)$_2$Mebpy-(CH$_2$)$_n$-MebpyRu(II)(bpy)$_2$ or Ru(II)(bpy)$_2$Mebpy-(CH$_2$)$_n$-Mebpy as impurities was found to be less than 0.5%. (vide infra).

The redox and electronic properties of **1** in the ground state was compared with those of its component complexes, (4,4′-dimethyl-2,2′-bipyridine)bis(2,2′-bipyridine)osmium(II), **5**, and -ruthenium(II), **6**, and a 1:1 mixture of **5** and **6**. Redox potentials in acetonitrile (MeCN) were measured by cyclic voltammetry using a glassy carbon or a platinum electrode. As an illustration, a cyclic voltammogram of **1** (n=3) is shown in Fig. 1. Irrespective of the number of methylene chains, **1** shows two reversible oxidation waves at 0.78 and 1.22 V vs. SCE for the Os(III)/Os(II) and Ru(III)/Ru(II) couples, which correspond to those of **5** and **6**, respectively. The peak-to-peak splitting for these waves is 60—70 mV, indicating that in **1**, two successive one-electron oxidation processes take place. A typical absorption spectrum for **1** (n=3) in methanol is shown in Fig. 2. As showm in Fig. 2, the electronic absorption spectrum of **1** (n=3) is identical with the superimposed spectrum of equimolar **5** and **6**. This was also observed in **1** (n=2,5, and 7). Thus, a comparison for the redox and electronic properties of **1** with its component complexes gave no evidence of an interaction between the ruthenium and osmium moieties of **1** in the ground state. This represents a marked difference from the covalently linked porphyrin dimers, in which the interaction between the porphyrin rings has been reported.[14,15]

The luminescence spectra of **1** (excitation wavelength: 455 nm) was recorded with an argon-gas bubbled methanol solution at room temperature and compared with that of a 1:1 mixture of **5** and **6** at the same substrate concentration. The efficient quenching of emission at 615 nm from a ruthenium complex and the enhancement of emission intensity at 730 nm from osmium complex were observed in **1** (n=3). In a mixture of **5** and **6**, no such quenching process could be observed because of the low substrate concentration (Fig. 3). For all **1** systems, a comparison of the spectra given in Fig. 4 shows that the degrees of quenching at 615 nm and sensitization at 730 nm increase in shorter

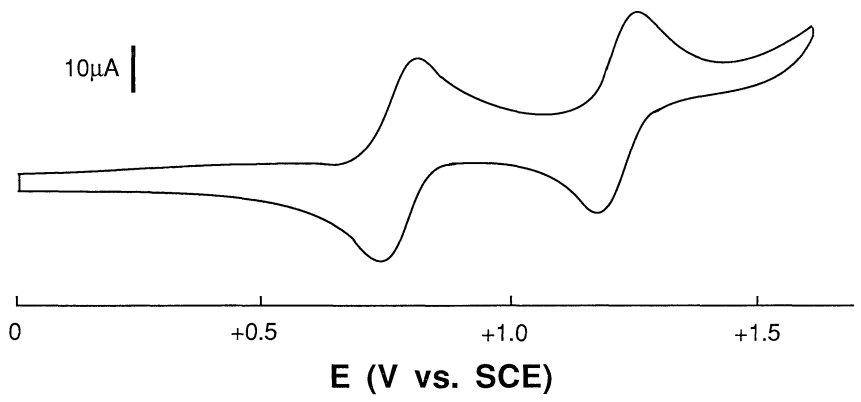

Fig. 1. Cyclic voltammogram of **1** (n=3) (1 mM) in MeCN solution with n-Bu$_4$NClO$_4$ as supporting electrolyte at a Pt disc electrode. Sweep rate was 200 mV s^{-1}.

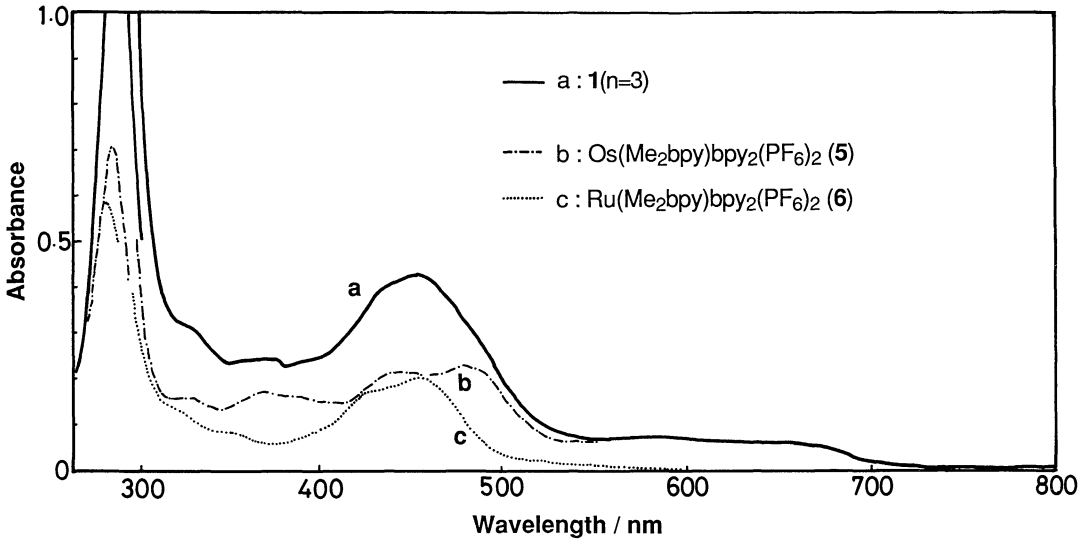

Fig. 2. Absorption spectra in water for **1** (n=3) (a), **5** (b), and **6** (c). [substrate]=1.5×10^{-5} M.

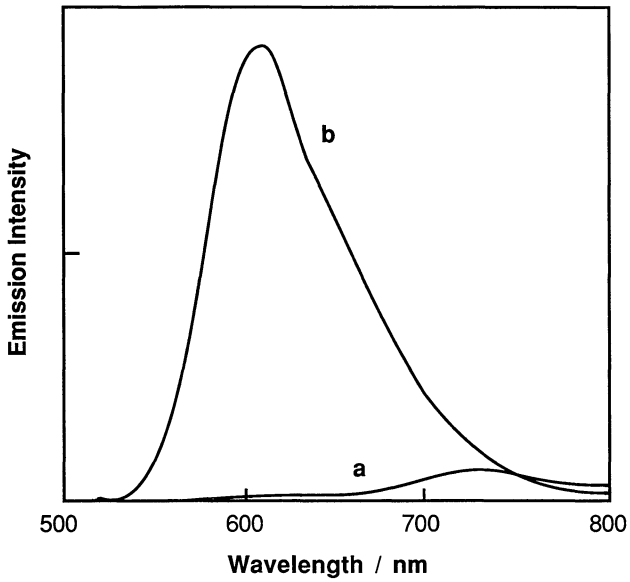

Fig. 3. Emission spectra of **1** (n=3) (a) and [**5**+**6**] (b) in MeOH. [substrate]=1.5×10^{-5} M. Excitation at 455 nm.

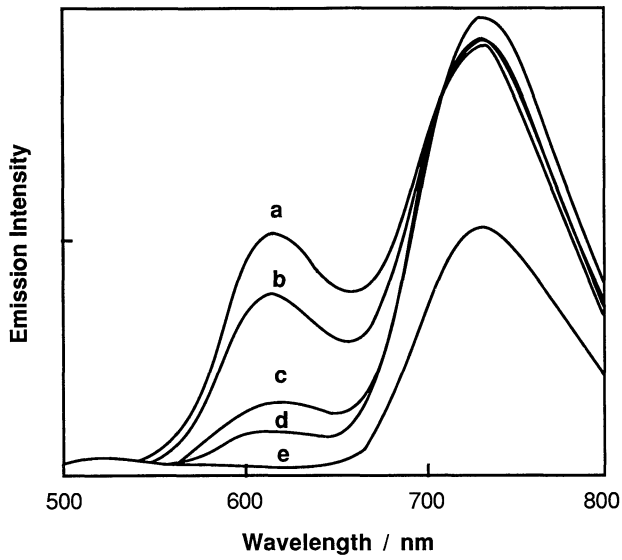

Fig. 4. Emission spectra of **1** in MeCN. [substrate]= 1.5×10^{-5} M. Excitation at 455 nm. **1** (n=7) (a), **1** (n=5) (b), **1** (n=3) (c), and **1** (n=2) (d). (e): The estimated contribution due to the direct excitation of osmium complex.

methylene chains. The molar absorption coefficients of **5** and **6** at 455 nm are equal. This overlap of absorption endows the equal probability of excitation of the Ru and Os moieties in **1**. In Fig. 4, spectrum e reveals the contribution due to a direct excitation of an osmium complex of **1** at 455 nm. The enhancement of emission at 730 nm indicates that the sensitization of the osmium complex by an excited ruthenium complex occurs through an intramolecular process in **1**.

As for the quenching mechanism, energy transfer from *Ru(II) to Os(II) and reductive electron transfer from Os(II) to *Ru(II) are conceivable. In acetonitrile, the first reduction potential of the $Ru^{2+/+}$ couple is -1.39 V, and the first oxidation potential of the $Os^{3+/2+}$ couple is 0.78 V vs.SCE (by cyclic voltammetry). Since substitution of one bpy-ligand of $Ru(bpy)_3^{2+}$ and $Os(bpy)_3^{2+}$ with 4,4′-dimethyl-2,2′-bipyridine does not show a marked difference in the absorption and emission maxima, the excited energies of the Ru-complex and the Os-complex of **1** can be assumed to be almost the same as those of $Ru(bpy)_3^{2+}$ and $Os(bpy)_3^{2+}$, respectively. The excited-state energy of the Ru-complex and the Os-complex of **1** were estimated to be 2.10[32] and 1.78 eV,[33] respectively. The photophysical behavior of **1** can be described in terms of an energy level diagram that is simply made by superimposing the low-lying excited states of the $Ru(bpy)_3^{2+}$ and $Os(bpy)_3^{2+}$ units on

the redox potentials in the ground state. The reductive quenching of the excited Ru-complex is slightly endergonic (ΔG=0.07 eV) based on a comparison of the reduction potential (0.71 V) for the $Ru^{2+*/+}$ couple with the oxidation potential (0.78 V) for the $Os^{3+/2+}$ couple. On the other hand, energy transfer can be more favorable by 0.32 eV, which corresponds to the observed difference in the emission maxima of the Ru-complex (E_{em}=1.63×10⁴cm⁻¹) and the Os-complex (E_{em}=1.37×10⁴ cm⁻¹) of **1**. The thermodynamical aspect allows us to conclude that energy transfer instead of electron transfer constitutes the quenching mechanism.

The occurrence of energy transfer can be detected by observing the enhancement of the emission intensity of the osmium chromophore along with a decrease in the emission intensity of the ruthenium chromophore. The decay of $Ru^{II}\rightarrow\pi^*$(bpy) MLCT emission at 610 nm and the rise and decay of $Os^{II}\rightarrow\pi^*$(bpy) MLCT emission at 800 nm were measured in various solvents by using a time-correlated single photon counting method[31] (excitation wavelength at 457.9 nm and instrumental width of 300 ps). Deconvolution of the luminescence profiles at 610 nm afforded the best fit by single exponential decay. In some cases, a minor, long-lived component was present (<0.5%). The amplitude of this component was sensitive to the degree of sample purification, it therefore most probably represents an impurity. Figure 5 shows the emission decay profile of an excited Ru-complex of **1** (n=7) in MeCN, with which a computer-calculated fit is superimposed. The fast exponential decay (12.1 ns: 8.3×10⁷ s⁻¹) is attributed to a deactivation of the ruthenium-excited state by an intramolecular energy transfer to the osmium complex. The double exponential analysis for the rise and decay of the excited-osmium complex at 800 nm gave 12 ns (8.3×10⁷ s⁻¹) for a rise corresponding to a decay of the excited ruthenium complex and 56 ns (1.8×10⁷ s⁻¹) for the decay, respectively. Table 1 contains the parameter

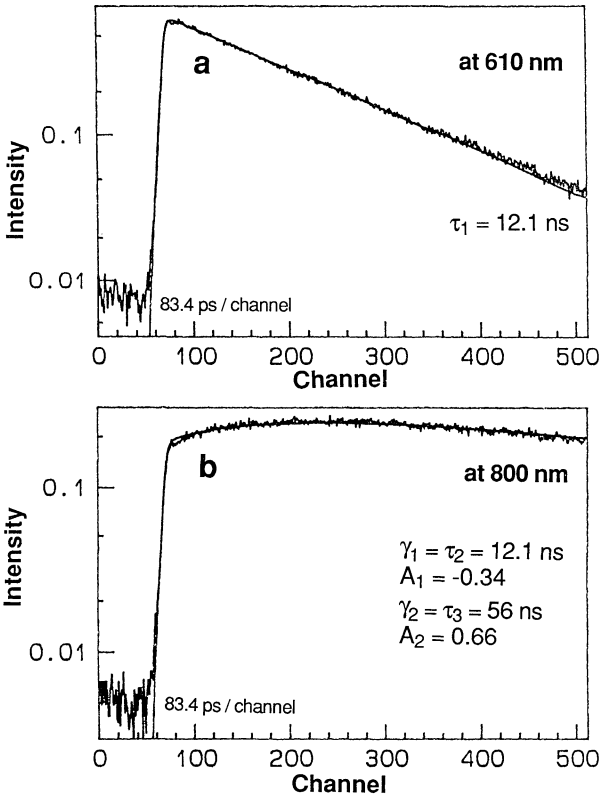

Fig. 5. Emission rise and decay for **1** (n=7) monitored at 610 nm (a) and 800 nm (b). 83.4 ps/channel, [**1**]=1×10⁻⁴M, solvent: MeCN.

Table 1. Emission Lifetimes and Energy-Transfer Rates[a]

Complex	Solvent	τ_1/ns[b]	τ_2/ns[c]	τ_3/ns[c]	k_{en}/s⁻¹[d]
1 (n=2)	H_2O	0.86[e]	0.93 (−0.25)	23 (0.75)	1.1×10⁹
	EtOH	1.9	1.9 (−0.33)	52 (0.67)	5.3×10⁸
	MeCN	1.2	1.2 (−0.38)	55 (0.62)	8.3×10⁸
1 (n=3)	H_2O	2.2	2.2 (−0.32)	18 (0.68)	4.5×10⁸
	EtOH	3.0	3.0 (−0.35)	37 (0.65)	3.3×10⁸
	MeCN	2.5	2.5 (−0.35)	44 (0.65)	4.0×10⁸
1 (n=5)	H_2O	5.8	5.8 (−0.35)	19 (0.65)	1.7×10⁸
	EtOH	8.0	8.0 (−0.36)	42 (0.64)	1.3×10⁸
	MeCN	7.9	7.9 (−0.33)	48 (0.67)	1.3×10⁸
1 (n=7)	H_2O	8.1	8.1 (−0.32)	20 (0.68)	1.2×10⁸
	EtOH	9.6[e]	10 (−0.36)	42 (0.64)	1.0×10⁸
	MeCN	12.1	12 (−0.34)	56 (0.66)	8.1×10⁷
3	H_2O	2.2	2.2 (−0.33)	19 (0.67)	4.5×10⁸
	EtOH	3.0	3.0 (−0.34)	41 (0.66)	3.3×10⁸
	MeCN	2.5	2.5 (−0.31)	41 (0.69)	4.0×10⁸
4	H_2O	1.1	1.1 (−0.32)	22 (0.68)	9.1×10⁸
	EtOH	1.9	1.9 (−0.34)	53 (0.66)	5.3×10⁸
	MeCN	1.4	1.4 (−0.32)	63 (0.68)	7.1×10⁸

a) All data represent averages and were measured at room temperature. The errors are less than 10%. b) Emission at 610 nm. c) Emission at 800 nm; the number in parenthesis indicates preexponential factors A_1 and A_2 for double exponential fit. d) Calcd from $1/\tau_1-1/\tau_0$; τ_0 is a lifetime of **6**. Values are 518, 729, and 859 ns in H_2O, EtOH, and MeCN, respectively. e) Average value of double exponential decay.

for the fit.

The excitation of **1**, denoted by Ru–C_n–Os at 457.9 nm, affords two excited states, namely *Ru–C_n–Os and Ru–C_n–Os* (Eq. 1a and 1b). In addition to the normal deactivation process (Eq. 1c and 1f), the reductive quenching of *Ru–C_n–Os by an intramolecular electron transfer process (Eq. 1d) and the buildup of Ru–C_n–Os* by the intramolecular energy transfer process (Eq. 1e) are taken into account:

$$\text{Ru–C}_n\text{–Os} \xrightarrow{h\nu} \text{*Ru–C}_n\text{–Os}, \quad (1a)$$

$$\text{Ru–C}_n\text{–Os} \xrightarrow{h\nu} \text{Ru–C}_n\text{–Os*}, \quad (1b)$$

$$\text{*Ru–C}_n\text{–Os} \xrightarrow{k_1} \text{Ru–C}_n\text{–Os} + (h\nu + \Delta), \quad (1c)$$

$$\text{*Ru–C}_n\text{–Os} \xrightarrow{k_{el}} \text{Ru–C}_n\text{–Os}, \quad (1d)$$

$$\text{*Ru–C}_n\text{–Os} \xrightarrow{k_{en}} \text{Ru–C}_n\text{–Os*}, \quad (1e)$$

and

$$\text{Ru–C}_n\text{–Os*} \xrightarrow{k_2} \text{Ru–C}_n\text{–Os} + (h\nu + \Delta). \quad (1f)$$

The relevant rate equations are

$$d[\text{*Ru–C}_n\text{–Os}]/dt = -(k_1 + k_{el} + k_{en})[\text{*Ru–C}_n\text{–Os}] \quad (2a)$$

and

$$d[\text{Ru–C}_n\text{–Os*}]/dt = k_{en}[\text{*Ru–C}_n\text{–Os}] - k_2[\text{Ru–C}_n\text{–Os*}] \quad (2b)$$

Equation (2b) yields

$$[\text{Ru–C}_n\text{–Os*}] = A_1\exp(-\gamma_1 t) + A_2\exp(-\gamma_2 t), \quad (3)$$

where $A_1=k_{en}[\text{*Ru–C}_n\text{–Os}]_0/(\gamma_2-\gamma_1)$, $A_2=[\text{Ru–C}_n\text{–Os*}]_0-A_1$, $\gamma_1=k_1+k_{el}+k_{en}$, $\gamma_2=k_2$, and $[\text{*Ru–C}_n\text{–Os}]_0$ and $[\text{Ru–C}_n\text{–Os*}]_0$ denote the initial concentration. γ_1 can be obtained from the decay time at 600 nm and the rise time at 800 nm. γ_2 can be also obtained from the decay time at 800 nm. The values of k_2 calculated from τ_3 $(=1/\tau_2)$ in Table 1 are of the order of $2—5\times10^7$ s^{-1}. The value of k_1 is 2×10^6 s^{-1} based on the lifetime of **6**.

Since the molar absorption coefficients of **5** and **6** at 457.9 nm are quite similar, we can deduce $[\text{*Ru–C}_n\text{–Os}]_0=[\text{Ru–C}_n\text{–Os*}]_0$. The ratio of the preexponential factors is given by

$$A_2/A_1 = (k_2 - k_1 - k_{el})/k_{en} - 2. \quad (4)$$

As indicated in Table 1, the A_2/A_1 values from the parameter for the computer fits of the experimental rise, and the decay profiles at 800 nm are close to -2. Equation 4 yields $(k_2-k_1-k_{el})/k_{en}\approx0$. Since k_2 is of the order of $2—5\times10^7$ s^{-1} and k_1 is 2×10^6 s^{-1}, k_{el} can be estimated to be of the order of 10^7 s^{-1} or less. The values of γ_1 $(=k_1+k_{el}+k_{en})$ calculated from τ_1 in Table 1 are $8—1\times10^8$ s^{-1}. By combining the estimated values of k_1 and k_{el}, k_{en} is found to be of the order of 10^8 s^{-1}; thus, $k_{en}\gg k_{el}$. This implies that the quantum efficiency of the energy transfer is almost 1, irrespective of the length of the methylene chain examined in the present study. Accordingly the electron transfer process by reductive quenching can be ruled out regarding **1**.

The rate constant, k_{en}, of energy-transfer can then be calculated via

$$k_{en} = k_{obs} - k_1, \quad (5)$$

where k_{obs} and k_1 can be calculated from the observed lifetime (τ_1) at 610 nm and the emission lifetime of **6**, $Ru(bpy)_2(dmb)^{2+}$(dmb=4,4′-dimethyl-2,2′-bipyridine), respectively. As presented in Table 1, k_{en} depend strongly on the length of the methylene chain, and increase in shorter methylene chains. Two mechanisms are possible for the present energy-transfer. The Förster mechanism operates via a dipole–dipole interaction between the transition moment and, therefore, requires no direct contact between the energy donor and acceptor. The Dexter mechanism depends upon the electron exchange and, thus, requires a spatial overlap. Discrimination between the Förster and the Dexter mechanisms can be achieved by studying the effect of varying the donor–acceptor separation (R). The rate constant for the Förster dipole–dipole transfer is expected to fall off with the inverse sixth power of R. The rate constant of the Dexter transfer, however, is predicted to parallel any decrease in the electronic overlap with increasing R, which may approximated by an exponential function. Although it is admittedly difficult to estimate the distance of **1** (n=2), space-filling molecular models indicate that, by using the molecular radius 4.7 Å of $Ru(bpy)_3^{2+}$ and assuming a fully extended trans-conformation for alkane bridges of the bridging

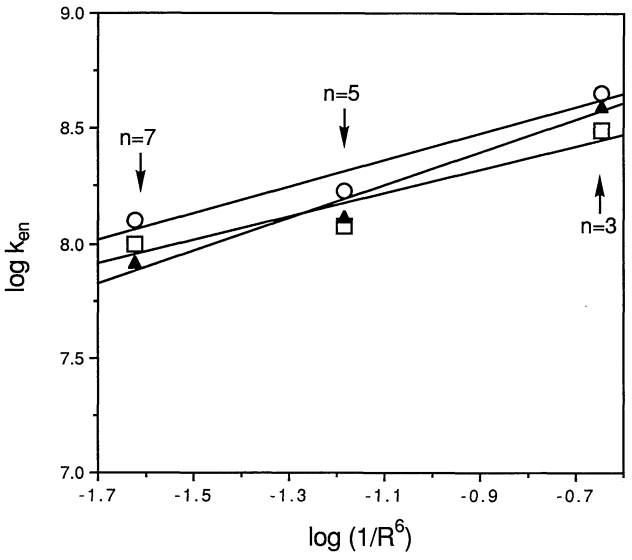

Fig. 6. Dependence of the rate of energy transfer on distance in various solvents. ○: in H_2O, ▲: in EtOH, and □: in MeCN.

ligands, the center-to-center separation distances in **1** are 12.8, 15.8, and 18.6 Å for n=3,5, and 7, respectively. It is adequate to evaluate R for a dipole–dipole interaction with a center-to-center rather than an edge-to-edge distance of both metal complexes. As shown in Fig. 6, the distance dependence of k_{en} in series **1** in water, ethanol, and acetonitrile can be fitted to an inverse sixth power law of the Förster mechanism. Instead, a steep drop of the rate is predicted by the Dexter mechanism in which k_{en} is expressed via an exponential dependence on the distance. Plots of the rate (k_{en}) vs. exp ($-R$) could not give a linear ralationship. These observations led us to conclude that a Förster-type interaction mechanism is operating in the intramolecular energy transfer in **1**.

A quantitative treatment of the Förster mechanism leads to the following expression for k_{en};[23]

$$k_{en} = \frac{9000 \ln 10 \kappa^2 \phi_D}{128\pi^5 n^4 N \tau_D R^6} \int_0^\infty F_D(\nu)\varepsilon_A(\nu)\frac{d\nu}{\nu^4} \qquad (6)$$

Here, ν is the wave number, $F_D(\nu)$ is the spectral distribution of the donor emission in quanta normalized to unity, $\varepsilon_A(\nu)$ is the molar extinction coefficient for the acceptor absorption, n is the refractive index of the solvent, κ is an orientation factor which equals $(2/3)^{1/2}$ for a random distribution of donor and acceptor molecules, ϕ_D is the quantum yield of donor emission, τ_D is the actual donor emission lifetime, N is Avogadro's number, and R is the distance between the donor and acceptor molecules. The overlap integral was calculated from numerical integration over the emission of **6** and the absorption of **5** in water and the value was 5.57×10^{-11} mol^{-1} cm^6. Based on the observed values of ϕ_D=0.028 and τ_D=4.77×10^{-7} s and assuming κ^2=2/3 and R=12.8 Å for **1** (n=3), the calculated k_{en} value was 1.4×10^8 s^{-1}, which was reasonably close to the observed value (4.5×10^8 s^{-1}).

Creutz and Sutin reported that the bimolecular quenching rate constant between excited $Ru(bpy)_3^{2+}$ and $Os(bpy)_3^{2+}$ was 1.5×10^9 M^{-1} s^{-1}, and that the reaction is almost diffusion-controlled.[34] The observed first-order rate constant for **1** seemed unexpectedly small. This fact might result from an electrostatic repulsion between two chromophores of **1**, which prevents any collisional quenching process based on an electron exchange (Dexter mechanism). It has been known that the intramolecular electron transfer via collisional processes in a trimethylene-linked donor-acceptor is influenced the solvent viscosity.[35] The dependence of solvent viscosity on the energy transfer rate (k_{en}) was examined for **1** (n=5) in three different solvents [ethanol(0.012), ethylene glycol (0.17), and glycerol (10.7) (in parentheses: viscosity in poise)]. In spite of the large difference in the viscosity, the observed k_{en} were in good agreement, that is, $(1.1—1.2)\times10^8$ s^{-1} irrespective of the solvent used. This finding also supports the Förster mechanism.

As shown in Table 1, a remarkable difference of k_{en} between **3** and **4** exists. According to the Förster formulation (Eq. 6), the rate constant is proportional to the spectral overlap and the reciprocal value of the radiative lifetime. The emission maxima (E_{em}), quantum yields (ϕ_{em}) and emission lifetime in water are 1.63×10^4 cm^{-1}, 0.028, and 477 ns for $Ru(bpy)_2(dmb)^{2+}$ and 1.61×10^4 cm^{-1}, 0.023, and 333 ns for $Ru(dmb)_3^{2+}$, respectively, which correspond to the ruthenium complex of **3** and **4**. Hence, the true radiative lifetimes are 17.0 μs for $Ru(bpy)_2(dmb)^{2+}$ and 14.5 μs for $Ru(dmb)_3^{2+}$. These values can not explain the observed differences. It is known that the excited electron in MLCT excited state of $Ru(bpy)_3^{2+}$ is fully localized on one of three equivalent ligands, at least for a time long enough for this ligand and its neighboring solvent to adjust to the geometry of fully charged bpy^-. Vibrational relaxation and localization have been suggested to come to completion within a few picoseconds.[36] In **3**, optical electron may preferentially reside on a bridging ligand rather than on a bpy ligand. On the contrary, the MLCT transition involves the π^* orbital of dmb ligands, rather than a bridging ligand in **4**. The orientation of the MLCT transition in **4** is possibly more favorable for the dipole–dipole interaction.

In the Förster mechanism, the mutual orientation of donor and acceptor complexes is important for determining the energy transfer rate. The polypyridine complex has two configurational isomers, namely Δ and Λ-isomers. It has been recognized that the dimer of polypyridine ruthenium complex, **2** (n=3), consists of a 1:1 diastereomeric mixture of (Δ-Δ) and (Δ-Δ+Λ-Λ).[12] **1** is also assumed to have the same composition of configurational isomers. A careful examination of the decay profiles indicates that there is no marked difference in the rate of the intramolecular energy transfer between these configurational isomers. Solvation may also cause a conformational change. The binuclear complex, **3** has an OH group on the bridging ligand. Protic solvents may interact with the OH group of **3**. Since the photophysical behavior of **1** (n=3) and **3** is quite the same, such an interaction is not important for intramolecular energy transfer.

It can be concluded that electrostatic repulsion prevents any collisional interaction between two chromophores of **1**, and that the dipole–dipole interaction is the main pathway for intramolecular energy transfer. The structural difference due to the configuration (Δ and Λ) of each chromophores is not important in the intramolecular energy transfer in the present case.

References

1) T. J. Meyer, *Acc. Chem. Res.*, **22**, 163 (1989).
2) D. Gust and T. A. Moore, *Science*, **244**, 35 (1989).
3) J. R. Norris, Jr. and D. Meisel, "Photochemical Energy Conversion," Elsevier, New York (1989), pp. 366.

4) M. A. Fox and M. Chanon, "Photoinduced Electron Transfer," Elsevier, Amsterdam (1988).
5) V. Balzani, "Supramolecular Photochemistry," D. Reidel Publishing Co., Doedrecht (1987).
6) R. Duesing, G. Tapolsky, and T. J. Meyer, *J. Am. Chem. Soc.*, **112**, 5378 (1990).
7) K. S. Schanze and L. Cabana, *J. Phys. Chem.*, **94**, 2740 (1990).
8) A. Osuka, K. Maruyama, N. Mataga, T. Asahi, I. Yamasaki, and N. Tamai, *J. Am. Chem. Soc.*, **112**, 4958 (1990).
9) D. Gust, T. A. Moore, A. L. Moore, S. Lee, E. Bittersmann, D. K. Luttrull, A. A. Rehms, J. M. DeGraziano, X. C. Ma, F. Gao, R. E. Belford, and T. T. Trier, *Science*, **248**, 199 (1990).
10) G. Tapolsky, R. Duesing, and T. J. Meyer, *Inorg. Chem.*, **29**, 2285 (1990).
11) K. Sumi, M. Furue, and S. Nozakura, *J. Polym. Sci., Polym. Chem. Ed.*, **23**, 3059 (1985).
12) M. Furue, N. Kuroda, and S. Nozakura, *Chem. Lett.*, **1986**, 1209.
13) J. B. Birks, "Photophysics of Aromatic Molecules," Wiley-Interscience, New York (1970).
14) Y. Kaizu, H. Maekawa, and H. Kobayashi, *J. Phys. Chem.*, **90**, 4234 (1986).
15) O. Ohno, Y. Ogasawara, M. Asano, Y. Kajii, Y. Kaizu, K. Obi, and H. Kobayashi, *J. Phys. Chem.*, **91**, 4269 (1987).
16) M. Furue, N. Kuroda, T. Yoshidzumi, S. Shun-ichi Nozakura, M. Kamachi, T. Ohno, W. E. Jones, Jr., and T. J. Meyer, *Polym. Prepr. Jpn.*, **38**, 1814 (1989).
17) C. A. Bignozzi, M. T. Indelli, and F. Scandola, *J. Am. Chem. Soc.*, **111**, 5192 (1989).
18) R. H. Schmehl, R. A. Auerbach, and W. F. Wacholtz, *J. Phys. Chem.*, **92**, 6202 (1988).
19) C. K. Ryu and R. H. Schmehl, *J. Phys. Chem.*, **93**, 7961 (1989).
20) R. Sahai, D. A. Baucom, and D. P. Rillema, *Inorg. Chem.*, **25**, 3843 (1986).
21) A. A. Lamola, "Energy Transfer and Organic Photochemistry," Interscience, New York (1969), pp. 17.
22) N. J. Turro, "Modern Molecular Photochemistry," The Benjamin/Cummings, Menlo Park, California (1978).
23) Th. Förster, *Discuss. Faraday Soc.*, **27**, 7 (1959).
24) D. L. Dexter, *J. Chem. Phys.*, **21**, 836 (1953).
25) F. Felix, J. Ferguson, H. U. Guedel, and A. Ludi, *J. Am. Chem. Soc.*, **102**, 4096 (1980).
26) E. M. Kober and T. J. Meyer, *Inorg. Chem.*, **23**, 3877 (1984).
27) M. Furue, S. Kinoshita, and T. Kushida, *Chem. Lett.*, **1987**, 2355.
28) K. Sumi, M. Furue, and S. Nozakura, *J. Polym. Sci., Polym. Chem. Ed.*, **22**, 3779 (1984).
29) F. B. Bohlmann, H. Bornowski, and P. Herbst, *Chem. Ber.*, **93**, 1931 (1960).
30) R. H. Schmehl, R. A. Auerbach, W. F. Wacholtz, C. M. Elliott, R. A. Freitag, and J. W. Merkert, *Inorg. Chem.*, **25**, 2440 (1986).
31) S. Kinoshita and T. Kushida, *Anal. Instrum.*, **14**, 503 (1985).
32) R. J. Watts, *J. Chem. Educ.*, **60**, 834 (1983).
33) C.-T. Lin and N. Sutin, *J. Phys. Chem.*, **80**, 97 (1976).
34) C. Creutz, M. Chou, T. L. Netzel, M. Okumura, and N. Sutin, *J. Am. Chem. Soc.*, **102**, 1309 (1980).
35) S. Russo and P. J. Thistlethwaite, *Chem. Phys. Lett.*, **106**, 91 (1984).
36) P. J. Carroll and L. E. Brus, *J. Am. Chem. Soc.*, **109**, 7613 (1987).